



1 Competing multiple oxidation pathways shape 2 atmospheric limonene-derived organonitrates simulated 3 with updated explicit chemical mechanisms

4 Qinghao Guo¹, Haofei Zhang², Bo Long³, Lehui Cui¹, Yiyang Sun¹, Hao Liu¹, Yaxin
5 Liu¹, Yunting Xiao¹, Pingqing Fu¹ and Jialei Zhu^{1,*}

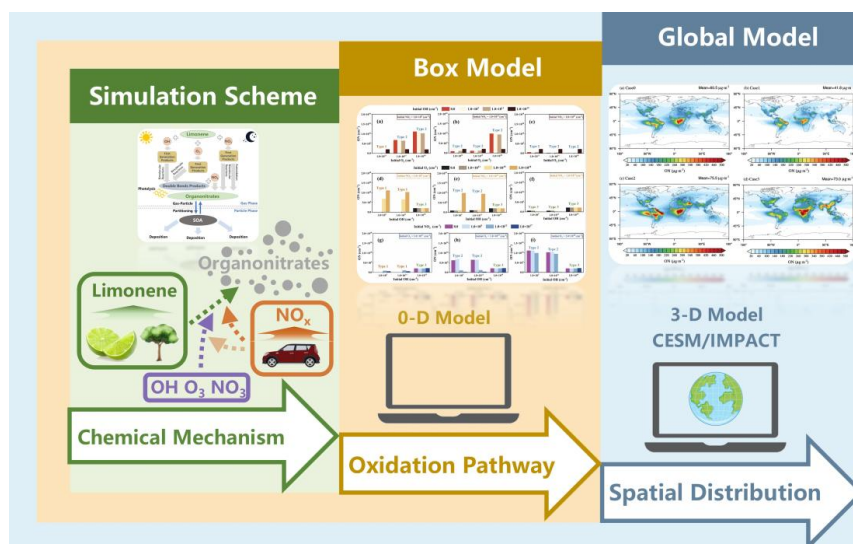
6 ¹ Institute of Surface-Earth System Science, School of Earth System Science, Tianjin University, Tianjin, 300072, China;

7 ² Department of Chemistry, University of California, Riverside, California 92521, USA;

8 ³ College of Materials Science and Engineering, Guizhou Minzu University, Guiyang 550025, China.

9 Correspondence to: Jialei Zhu, Email: zhujialei@tju.edu.cn

10 **Abstract.** Organonitrates (ON) are key components of secondary organic aerosols (SOA) with potential
11 environmental and climate effects. However, ON formation from limonene, a major monoterpene, and
12 its sensitivity to oxidation pathways remain insufficiently explored due to the absence of models with
13 explicit chemical mechanisms. This study advances the representation of limonene-derived ON
14 formation by incorporating 90 gas-phase reactions and 39 intermediates across three oxidation pathways
15 (O_3 , OH, NO_3) into both a chemical box model and a global model. Box model sensitivity experiments
16 revealed that competition among major oxidation pathways, coupled with the high yield of limonene-
17 derived ON from O_3 -initiated oxidation, leads to increased limonene-derived ON production when the
18 O_3 -initiated pathway is enhanced, whereas strengthening the OH- or NO_3 -initiated pathways reduces ON
19 formation. Compared to the box model, the global simulation exhibits stronger nonlinear responses and
20 great spatiotemporal variability in limonene-derived ON formation across different oxidation pathways.
21 This is primarily driven by the complex distribution of precursors and oxidants, as well as changing in
22 dominate chemical pathways under various meteorological conditions. In the presence of the other two
23 pathways, increasing the O_3 - or NO_3 -initiated oxidation pathway reduces the global limonene-derived
24 ON burden by 19.9% and 17.3%, respectively, whereas enhancing the OH-initiated pathway increases it
25 by 44.7%. limonene-derived ON chemistry developed in this study not only enhances the global model's
26 ability to simulate ON formation evaluated through comparison with observations but also demonstrates
27 an approach based on explicit chemical mechanisms that establishes a methodological framework for
28 simulating the chemical formation processes of SOA.



29

30 1 Introduction

31 Secondary organic aerosols (SOA) represent a substantial fraction of fine particulate matter and
 32 contribute to global public health risk, deterioration of air quality and climate change (Collaborators,
 33 2024; Lelieveld et al., 2015; Tao et al., 2017). Among chemical constituents, organonitrates (ON) are of
 34 particular interest owing to their large fraction in SOA (5%-77%) (Farmer et al., 2010; Kiendler-Scharr
 35 et al., 2016). The rate of particulate ON formation contributes strongly to the rate of SOA formation at
 36 night, which emphasizes the important roles of particulate ON in ambient SOA (Guo et al., 2024). The
 37 nitrate group in ON would influence the physical and chemical properties of SOA, such as decreasing
 38 saturated vapor pressure of the product molecule (Capouet and Müller, 2006). ON are secondary
 39 compounds formed via the oxidation of volatile organic compounds (VOCs) in the presence of nitrogen
 40 oxides ($\text{NO}_x = \text{NO} + \text{NO}_2$), substantially influencing NO_x cycling and formation of ozone (O_3) and
 41 HONO (Perring et al., 2013). In global scale, VOCs are mainly emitted from biogenic sources, while
 42 NO_x are emitted from a wide variety of anthropogenic sources (Ng et al., 2017; Glasius and Goldstein,
 43 2016). Therefore, a thorough investigation of ON is warranted to advance our understanding of
 44 interaction between biogenic and anthropogenic emissions.

45 The chemical formation mechanisms of ON are complex, hampering efforts to simulate and control
 46 SOA. In the daytime, hydroxyl radicals (OH) and ozone (O_3) oxidation of VOCs can produce peroxy



radical (RO_2), which reacts with NO_x to produce ON (Perring et al., 2013), while the reaction between nitrate radicals (NO_3) and VOCs dominates the generation of ON in the nighttime (Rollins et al., 2009; Perring et al., 2013; Ng et al., 2017). Furthermore, the coexistence among OH, O_3 and NO_3 has been investigated in VOCs nocturnal oxidation (Brown and Stutz, 2012; Barber et al., 2018; Kwan et al., 2012; Chen et al., 2022). Compared with single oxidant, the introduction of multiple oxidants is evaded for the possible complex reaction mechanisms for VOCs. The regeneration of OH would change the O_3 oxidation process to form SOA (Sato et al., 2013). Chamber experiments show that SOA from NO_3 oxidation of VOCs are affected by oxidation of NO_2 by O_3 (Ng et al., 2017). Therefore, VOCs are oxidized through the synergistic effects of multiple oxidants, driving the chemical formation of ON. However, ON formation from the VOCs oxidation governed by mixing oxidants has not been fully understood. In particular, the impact of oxidation pathways on the ON formation and spatial distribution are still unclear.

As one of typical biogenic volatile organic compounds (BVOCs) (10% of monoterpenes), limonene is mostly emitted from citrus plants and coniferous trees, with a total emission rate of $\sim 11 \text{ Tg}\cdot\text{yr}^{-1}$ (Guenther et al., 2012; Sindelarova et al., 2014). Limonene has unique structure with an endocyclic double bond and an exocyclic double bond, which makes it reactive towards atmospheric oxidants (Surratt et al., 2008). Higher ON (30–72%) and SOA yields (17–40%) through NO_3 -initiated oxidation of limonene than other monoterpenes have been observed in laboratory experiments (Fry et al., 2014; Hallquist et al., 1999; Spittler et al., 2006; Moldanova and Ljungström, 2000; Fry et al., 2011). It has been well demonstrated that limonene + NO_3 is most important pathway to form limonene-derived ON (Kilgour et al., 2024; Ehn et al., 2014; Jokinen et al., 2015; Zhao et al., 2015). Furthermore, recent study found the primary nitrooxy RO_2 formed through NO_3 addition to limonene occurs at both at endocyclic double bond and the exocyclic double bond. These products could undergo autoxidation, which is fast enough to RO_2 bimolecular reactions (Mayorga et al., 2022). The molecular compositions and formation mechanism of limonene-derived ON have been well investigated through observations and laboratory studies, while their description in models remains not explicit and advanced.

The early atmospheric model utilizes empirical yields and empirical coefficients for predicting limonene-derived SOA production in simulation (Yu et al., 2019). Currently, chemical mechanisms are simplified according to analogies with structurally similar compounds in most of regional and global



models due to simplicity and efficiency in calculation (Fisher et al., 2016; Li et al., 2023a). Nevertheless, previous model studies have not included the formation mechanism of limonene-derived ON in detail (Pye et al., 2015; Li et al., 2023a; Zare et al., 2019). Simplified mechanisms make it difficult to understand explicit limonene-derived ON formation process and the influence of interaction between multiple oxidation pathways on ON formation.

Herein, we investigated the impacts of multiple oxidation pathways on limonene-derived ON using both chemical box model and global model, which were developed to include explicit chemical mechanisms for limonene-derived ON formation. The effect of competition among individual oxidation pathways on limonene-derived ON formation were discussed using a chemical box model based on proposed mechanisms. The simulation framework of explicit chemical mechanisms was integrated into global model to evaluate the spatial distributions of limonene-derived ON and contributions of individual oxidation pathways. This study presents a numerical simulation framework for atmospheric chemical processes and aims at enhancing the ability of models to simulate ON and understand the competition effects among atmospheric oxidation pathways on SOA formation, improving atmospheric composition forecasts and informing interaction between biogenic and anthropogenic emissions.

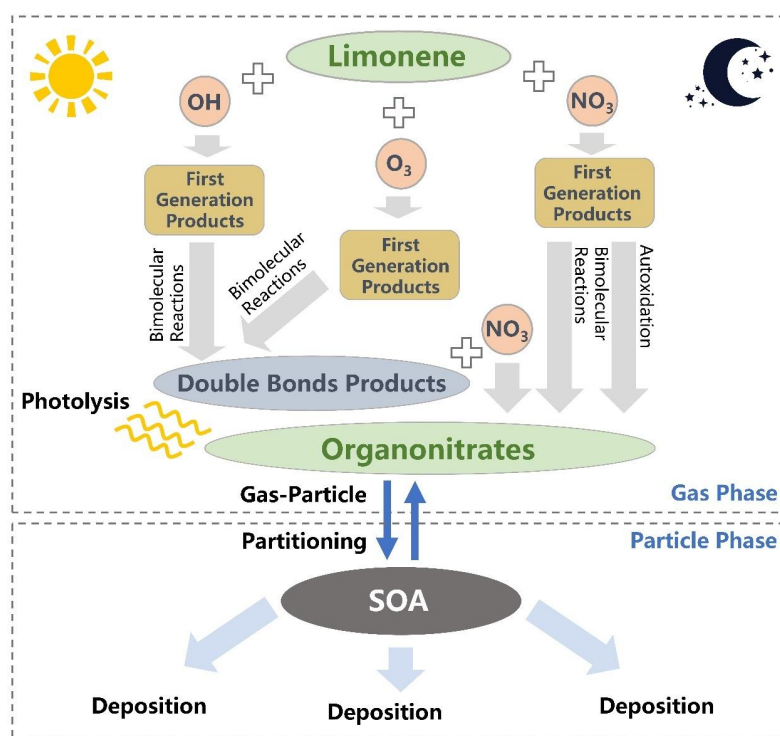
2 Methodology

2.1 Limonene-derived ON formation mechanism

In order to simulate ON via the gas-phase oxidation of limonene, the chemical mechanism used in our model was updated with gas-phase chemical mechanisms of limonene-derived ON based on recent laboratory studies (Mayorga et al., 2022) and Master Chemical Mechanism (MCM, v3.3.1). The explicit chemical mechanism of limonene-derived ON involves three initial oxidation pathways: OH-, O₃- and NO₃-initiated oxidation (Fig. 1). The detailed formulas of species could be found in Table S1. The updated explicit formation mechanisms were list in Fig. S1 and Table S2. Compared to the MCM mechanism, the chemical mechanism of limonene-derived ON formation used in this study is developed to include: (1) NO₃ addition at three different carbonsites. The branching ratios of the three C₁₀H₁₆NO₅-RO₂ isomers were estimated to 0.63:0.34:0.03 based on previous laboratory studies (Leungsakul et al., 2005; Wang and Wang, 2021). (2) Sequential NO₃ oxidation reactions to form ON for all the products that contain double bonds from OH- and O₃-initiated oxidation in MCM. The rate constants were set to



104 be the same as those used in MCM for limonene. (3) The formation of a ring-opened nitrooxy RO₂
105 in the presence of O₂ due to bond scission of the two endocyclic nitrooxy RO, and its branching ratio
106 was estimated (Draper et al., 2019; Kurten et al., 2017; Guo et al., 2022). (4) H-shifts of the exocyclic
107 C₁₀H₁₆NO₄-RO. (5) Bimolecular and unimolecular reactions of the C₁₀H₁₆NO₆-RO₂ and C₁₀H₁₆NO₇-RO₂.
108 The rate constants for the bimolecular reactions are the same as those used in MCM, and autoxidation
109 rate constants are calculated. In our explicit chemical mechanism, more intermediates and chemical
110 processes of limonene-derived ON were distinguished than simplified mechanisms used in previous
111 models.



112
113 **Figure 1.** Schematic diagram of the limonene-derived ON formation pathways included in this work.

114 We assumed highly oxidated ON products (C₁₀H₁₃NO₇, C₁₀H₁₅NO₄, C₁₀H₁₅NO₅, C₁₀H₁₅NO₆,
115 C₁₀H₁₅NO₇, C₁₀H₁₅NO₈, C₁₀H₁₇NO₅, C₁₀H₁₇NO₆, C₁₀H₁₇NO₇) to be semi- to low-volatile which can
116 condense into the particulate phase upon formation. Their vapor pressures are estimated to calculate gas-
117 particle partitioning (Table S3).



The vapor pressures of the above-mentioned ON species were estimated using the EVAPORATION method (Compernelle et al., 2011). It is one of the widely used group contribution-based models to predict molecular vapor pressures. As the model input, the structures of the ON species were obtained from prior work (Mayorga et al., 2022) and converted to SMILES strings. To validate the method, the predicted vapor pressures were also compared with another commonly used method, SIMPOL 1 (Pankow and Asher, 2008), which requires only the functional groups as inputs. The two methods predict vapor pressures within one order of magnitude in most cases, supporting our estimation.

2.2 Chemical box model

A zero-dimensional (0-D) chemical box model was used to examine the chemical processes of limonene-derived ON, investigating the contributions of atmospheric oxidants and oxidant pathways. The chemical mechanism presented in Fig. S1 and Table S2 was applied in this box model. To calculate the total production of limonene-derived ON, processes such as photolysis, dilution, and deposition were ignored for all chemical species in the model. The temperature was set to 298 K in the model. The initial concentrations of limonene and other atmospheric components for all cases were set as shown in Table S5. Limonene at a concentration of 1.0×10^{11} molecules·cm⁻³ was used as the precursor for ON (Guo et al., 2022; Luo et al., 2023). The initial concentration of OH, O₃ and NO₃ spanned 1.0×10^5 to 1.0×10^{19} molecules·cm⁻³, 1.0×10^{11} to 1.0×10^{18} molecules·cm⁻³ and 1.0×10^9 to 1.0×10^{17} molecules·cm⁻³, respectively. The low values represent typical atmospheric concentrations of these species, which are within the range of those reported in previous studies (Shen et al., 2021; Liu et al., 2023; Matsunaga and Ziemann, 2019). The medium to high values represent extreme conditions, in order to investigate the significant impact of oxidants on limonene-derived ON across a broad spectrum of oxidant levels. Chamber experiments were simulated by the box model under ideal situation, which has been specifically design to analyze chemical processes, while simulations under real atmospheric condition were carried using global model in sect. 2.3. We conducted sensitivity tests (Sect. S1 in the supplement) to examine oxidation pathways for formation of limonene-derived ON. Sensitivity tests under single initial oxidation were set. Building upon this foundation, sensitivity tests with multiple oxidation pathways were implemented: (1) introducing secondary oxidant across three concentration gradients under fixed primary oxidant levels, followed by (2) increasing concentration of third oxidant with three concentration gradients. A summary of all cases can be found in Table S4.



147 **2.3 Simulation of global limonene-derived ON**

148 We used the Community Earth System Model (CESM) version 1.2.2.1 coupled with the University of
149 Michigan Integrated Massively Parallel Atmospheric Chemical Transport (IMPACT) aerosol model with
150 a resolution of $1.9^\circ \times 2.5^\circ$ for this study. The IMPACT aerosol module gets the meteorology field from
151 the CESM model at each time step, while changes in the aerosols in IMPACT do not provide feedback
152 to the CESM. The emission of precursors BVOCs are estimated by the Model of Emissions of Gases and
153 Aerosols from Nature inventory (MEGAN) coupled to CESM/IMPACT model. The developed explicit
154 gas phase chemical mechanism same as used in above chemical box model was applied to simulate the
155 formation of limonene-derived ON. The highly oxidated limonene-derived ON considered as semi-
156 volatile species partitioning from gas phase to particle phase contributes to SOA. A base case (Case0)
157 was designed to simulate limonene-derived ON under all three initial oxidation pathways, and six
158 sensitivity experiments were designed for simulating global burden limonene-derived ON under two
159 initial oxidation pathways (Case 1-3) and single initial oxidation pathway (Case 4-6), respectively.
160 Above seven cases were summarized in Supplementary Sect. S2 and Table S6.

161 **3 Results and discussion**

162 **3.1 Limonene-derived ON formation through individual initial oxidation pathway.**

163 We employed a chemical box model to simulate limonene-derived ON formed through three initial
164 oxidation pathways, considering various oxidant concentrations (Fig. 2). These simulations were
165 designed to evaluate the effect of increasing oxidant concentrations on the yield of limonene-derived ON
166 from each initial oxidation pathway. In the case with individual OH oxidation pathway, the concentration
167 of limonene-derived ON increases as the initial OH concentration increases (Fig. 2a), following a pattern
168 to that of limonene consumption (Fig. S2a). Initial OH concentration increases from 1.0×10^5 to 1.0×10^{19}
169 molecules·cm⁻³, resulting in ~20.0-fold increase in the production of limonene-derived ON. At this stage,
170 limonene is not completely consumed by OH, indicating that higher initial OH concentration will
171 increase consumption of limonene to produce more ON.

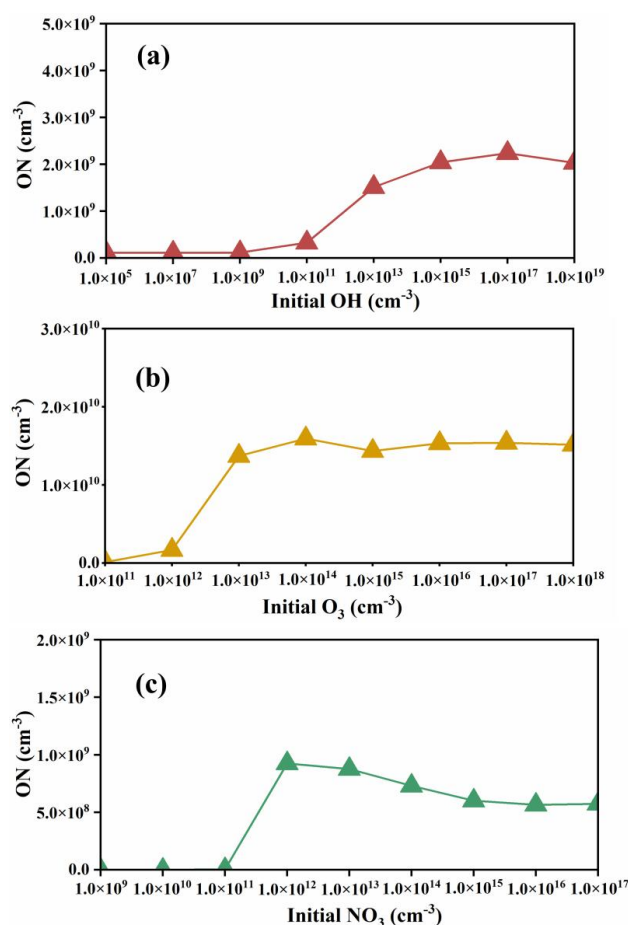


Figure 2. Variations of limonene-derived ON in individual oxidation pathway under different oxidant concentrations. The triangles represent concentration of limonene-derived ON in each experiment. The lines represent the trend of limonene-derived ON. The three datapoint colors represent three initial oxidation pathways (red for OH-initiated oxidation, yellow for O₃-initiated oxidation, green for NO₃-initiated oxidation).

In the case with individual O₃ oxidation pathway, the limonene-derived ON increases first and then maintains a relatively stable production with the increase of initial O₃ concentration (Fig. 2b). Limonene is not completely consumed when initial O₃ concentrations below 1.0x10¹⁴ molecules·cm⁻³. Increased consumption of limonene lead to an increase in ON production with increased O₃ concentration.

Different from the cases of the OH- and O₃-initiated oxidation pathways, limonene-derived ON increases when initial NO₃ concentrations below 1.0x10¹² molecules·cm⁻³ could be caused by incompletely consumed limonene (Fig. 2c). The increased consumption of limonene with increase in



184 concentrations of NO_3 lead to the increased production of ON. However, as initial NO_3 concentrations
185 continued to increase, limonene-derived ON production decrease. Compared to the case with initial NO_3
186 concentration of 1.0×10^{12} molecules cm^{-3} , reaction of LIMAL and NO_3 become the dominant pathway
187 in the case with initial NO_3 concentration of 1.0×10^{17} molecules $\cdot \text{cm}^{-3}$. Low yield (9.2%) of this pathway
188 results in decreased limonene-derived ON (green box in Fig. S1). The results mean that at low initial
189 oxidant concentration, limonene-derived ON shows a strong dependence on initial oxidant concentration,
190 and the dependence on intermediate reaction rates becomes more important at high initial oxidant
191 concentration.

192 In addition, average concentration of ON of OH^- , O_3 - and NO_3 -initiated oxidation pathways when
193 oxidations are sufficient are calculated separately. The O_3 -initiated oxidation pathway (1.5×10^{10}
194 molecules $\cdot \text{cm}^{-3}$ limonene-derived ON produced) yields more ON than the OH^- (2.1×10^9 molecules $\cdot \text{cm}^{-3}$
195 limonene-derived ON produced) and NO_3 -initiated (7.1×10^8 molecules $\cdot \text{cm}^{-3}$ limonene-derived ON
196 produced) oxidation pathways when limonene initial concentration is constant. This indicates that under
197 initial conditions with sufficient oxidation, O_3 -initiated oxidation pathway of limonene has highest yield
198 of ON, which is about 15.0%, while that is low by OH^- (2.1%) and NO_3 -initiated (0.7%) oxidation
199 pathway. This difference in the ON yield among various oxidation pathways will be used to explain the
200 contributions of each oxidation pathway to ON concentration in the following discussion.

201 **3.2 Effects of multiple oxidation pathways on limonene-derived ON formation.**

202 Compared to the simulation scheme with individual oxidation pathway discussed above, introducing
203 multiple oxidation pathways leads to comprehensive competition among them, which results in a
204 nonlinear response of ON concentration to changes in the initial concentrations of oxidants. Figure 3
205 shows the dependence of limonene-derived ON on initial concentration of oxidants when include two
206 initial oxidation pathways. The addition of oxidants has various effects on the yield of limonene-derived
207 ON. When the initial concentration of oxidant is low (1.0×10^5 molecules $\cdot \text{cm}^{-3}$ for OH^- , 1.0×10^{11}
208 molecules $\cdot \text{cm}^{-3}$ for O_3 , 1.0×10^9 molecules $\cdot \text{cm}^{-3}$ for NO_3), the initial limonene will not be completely
209 consumed. In all case with low concentration of oxidants, adding another oxidant with oxidation pathway
210 will increase consumption of limonene, leading to increase in the limonene-derived ON production.
211 When the initial concentration of oxidants is high, limonene will be nearly or completely consumed. In



212 these cases, the production of limonene-derived ON will be determined by the competition between the
213 two oxidation pathways. The product of limonene-derived ON steadily increased as the initial
214 concentration of O_3 increases from 0 to 1.0×10^{18} molecules·cm⁻³ when the initial concentration of OH or
215 NO_3 is constant (Fig. 3a, f). According to the chemical mechanism applied in the model, the reaction
216 between limonene and O_3 has higher rate than OH and NO_3 in these cases (Table S7). As a result, in the
217 presence of O_3 , the oxidation of limonene with O_3 proceeds more rapidly than with OH or NO_3 , leading
218 to higher concentration of limonene-derived ON due to the high yield of O_3 oxidation pathway as
219 discussed in above section (compare Fig. 2b with Fig. 2a and 2c). In contrast, compared to only including
220 O_3 oxidation pathway, adding oxidation pathways with OH or NO_3 will result in a decrease in limonene-
221 derived ON production (Fig. 3c, d), because some limonene that would have reacted with O_3 is instead
222 converted to ON through the OH or NO_3 pathways with lower yield. Therefore, the dominant oxidation
223 pathway and its ON yield determine the impact of the competition between the two oxidation pathways
224 on the final limonene-derived ON production. A similar phenomena observed in laboratory study shows
225 that NO_x influences γ -terpinene ozonolysis by enhancing NO_3 production at high NO_x levels, which
226 subsequently leads to NO_3 preferentially consuming γ -terpinene over O_3 (Xu et al., 2020), illustrating
227 the competition between oxidants. The addition of the OH-initiated oxidation pathway results in a small
228 increase in ON production compared to NO_3 -initiated oxidation alone (Fig. 3e), due to the slightly higher
229 yields of limonene-derived ON for OH-initiated oxidation pathway. The ON production would not
230 change much when add the NO_3 -initiated oxidation pathway compared to the case with OH-initiated
231 oxidation pathway alone (Fig. 3b) because of unchanged the main initial oxidation pathway. These
232 sensitivity experiments suggest that competition of oxidation pathways plays an important role in
233 formation of limonene-derived ON.

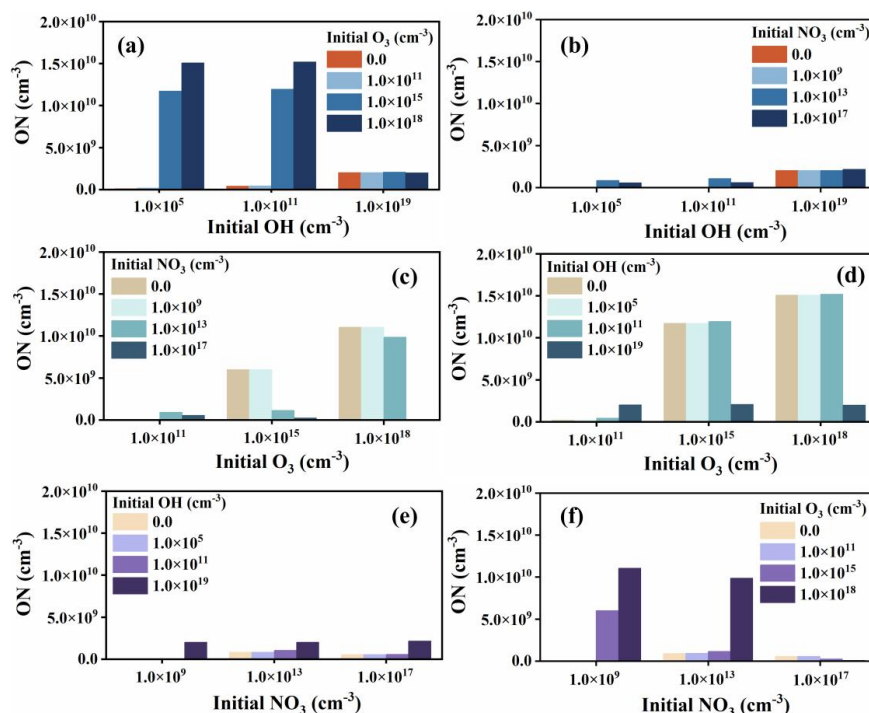
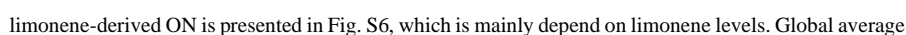


Figure 3. Simulated limonene-derived ON in two initial oxidation pathways under different oxidant conditions, including variation of production of limonene-derived ON with adding (a) initial O₃ concentration and (b) initial NO₃ concentration in the three OH levels; variation of limonene-derived ON production with adding (c) initial OH concentration and (d) initial NO₃ concentration in the three O₃ levels; variation of limonene-derived ON production with adding (e) initial OH concentration and (f) initial O₃ concentration in the three NO₃ levels.

Based on the production variations of limonene-derived ON in the cases with one and two initial oxidation pathways discussed above, the comprehensive impact of multiple oxidants on limonene-derived ON formation in the cases with multiple initial oxidation pathways are analyzed (Fig. 4). The results can be summarized into three types. The Type 1 is the cases when limonene is not completely consumed (Fig. S4). When two initial oxidant concentration is low (Fig. 4a, d, g) and medium (Fig. 4d, g), the addition of third oxidant increases the production of limonene-derived ON because the addition of the third oxidant increases consumption of limonene. If the oxidant concentration is sufficient to consume up limonene, the production of limonene-derived ON will be determined by the competition between initial oxidation pathways. The Type 2 is the cases with large changes of limonene-derived ON. Under low NO₃ and moderate and high O₃ conditions, the production of limonene-derived ON decreases with adding OH (Fig. 4a, b), because some limonene that would have reacted with O₃ is instead converted



251 to ON through the OH pathways with lower yield. The formation of limonene-derived ON shows similar
252 pattern for Type 2 in Figure 4h and i. On the one hand, the yield of limonene-derived ON from NO₃-
253 initiated oxidation is lowest, so the production of limonene-derived ON will decrease when the formation
254 of limonene-derived ON from this pathway becomes the dominant formation route. On the other hand,
255 adding NO₃-initiated oxidation pathway also consumes NO₃ that would have reacted with the product of
256 the OH- and O₃-initiated oxidation, resulting in decrease production of limonene-derived ON. The
257 changes in ON production with constant initial concentration of limonene and various oxidation
258 pathways indicate the interactions of different oxidation process of limonene. In contrast to OH- and
259 NO₃-initiated oxidation pathway, adding oxidation pathways with O₃ will result in increase in limonene-
260 derived ON production (Fig. 4e), due to higher yield of limonene-derived ON from O₃-initiated oxidation
261 pathway than OH- and NO₃-initiated oxidation pathways. Since the yield of limonene-derived ON of OH-
262 initiated oxidation is higher than NO₃-initiated oxidation, the production of limonene-derived ON
263 decreases (Fig. 4c) as the main oxidation pathway changes from NO₃ to OH oxidation (Table S8).
264 Additionally, in some sensitivity experiments (Fig. 4d-i), ON concentration do not change much with the
265 addition of an oxidation pathway (Type 3). This could be explained by minimal competition with the
266 rapid main oxidation pathway. These sensitivity experiments suggest that the limonene-derived ON
267 production in the simulated system are not only controlled by limonene concentration, but also affected
268 by synergic effect of multiple oxidants and oxidation pathways.





limonene-derived ON burden peaks in the summer ($69.2 \mu\text{g}\cdot\text{m}^{-2}$) due to highest global average limonene concentration (Fig. S7b), while the large burden of limonene-derived ON in fall is driven by the presence of both high limonene concentration (Fig. S7c) and NO concentration (Fig. S8c) compared to spring and winter. In contrast, the burden of limonene-derived ON is lowest in winter ($48.1 \mu\text{g}\cdot\text{m}^{-2}$) because of lowest concentration of limonene (Fig. S7d). Beyond the effects of limonene and NO concentrations, oxidant levels and oxidation pathways also affect the formation mechanisms and production of limonene-derived ON, which may explain the highest burden in regions such as Central Africa, rather than Amazon where limonene concentrations are highest over the world (Fig. S9a). The concentration of oxidants is inherently low in Amazon (Fig. S9b-d) and most oxidants are consumed by reaction with isoprene and some other monoterpene with higher concentrations compared to limonene. Consequently, only a few of oxidants are available to react with limonene, leading to low burden of limonene-derived ON in Amazon despite the highest burden of limonene there. Therefore, high concentrations of limonene-derived ON can only form when both high limonene and oxidant concentrations are present simultaneously.

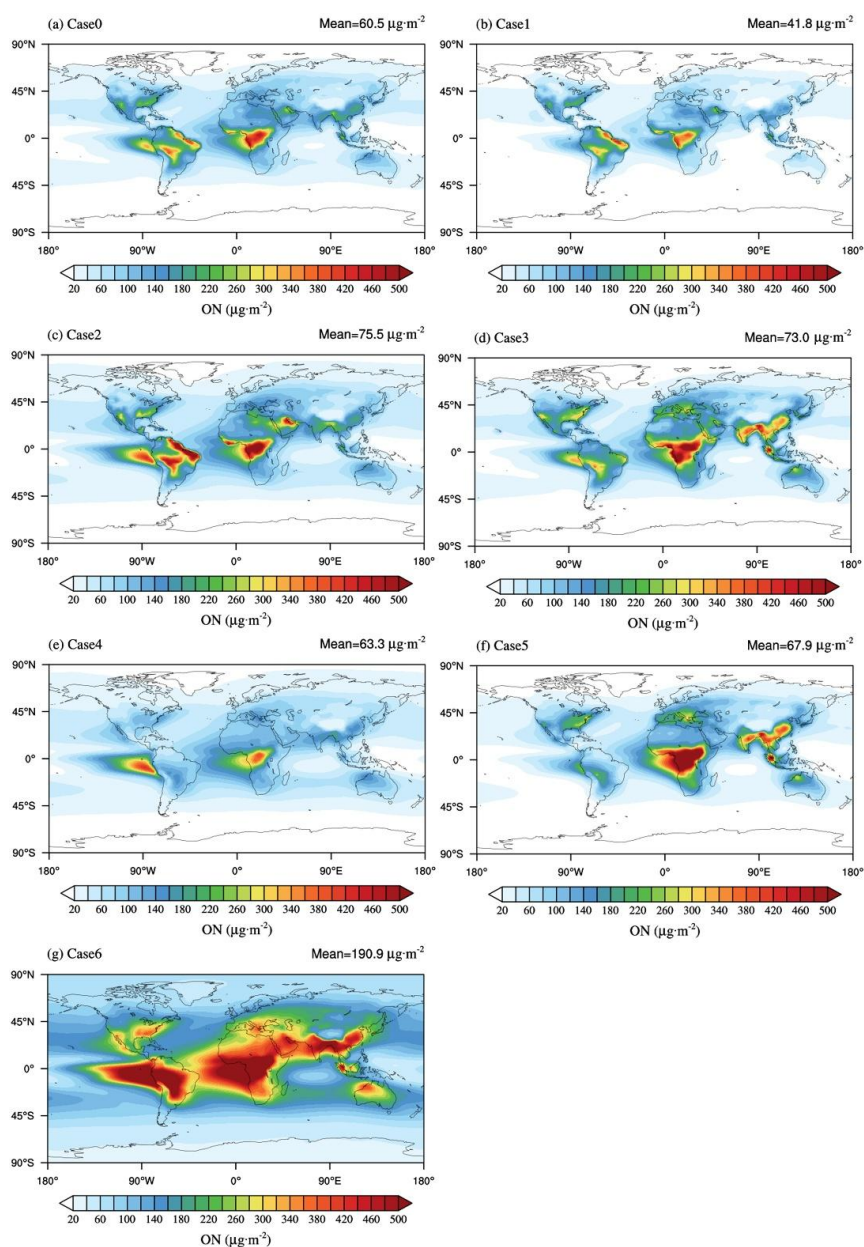


Figure 5. Annual mean column concentration of limonene-derived ON with different simulation schemes. (a) Run with three initial oxidation pathways (Case0), (b) without OH-initiated oxidation pathway (Case1), (c) without O₃-initiated oxidation pathway (Case2), (d) without NO₃-initiated oxidation pathway (Case3), (e) without O₃- and NO₃-initiated oxidation pathways (Case4), (f) without OH- and NO₃-initiated oxidation pathways (Case5) and (g) without OH- and O₃-initiated oxidation pathway (Case6).



307 To quantify the contribution of each oxidation pathway to the formation of limonene-derived ON in
308 different regions, we conducted a series of sensitivity experiments (Case1 to 6 introduced in method
309 section) on the oxidation pathways (Fig. 5b-g). Our simulations indicate that increasing O₃ and NO₃-
310 initiated oxidation pathways result in 15.5% and 18.0% increase of global average burden of limonene-
311 derived ON, respectively, compared to OH-initiated oxidation pathway alone (Fig. S10a, b). This is
312 primarily because higher yields of limonene-derived ON associated with the O₃- and NO₃-initiated
313 oxidation pathways compared to OH-initiated oxidation pathways. When compared to O₃-initiated
314 oxidation pathway alone (Fig. S10c, d), the addition of OH- or NO₃-initiated pathways result in increased
315 burden of limonene-derived ON in the limonene-sufficient region (e.g. Amazon), owing to adding a
316 limonene-derived ON formation pathway to consume more limonene. However, in the limonene-
317 deficient yet NO₃-sufficient regions (e.g. Central Africa, Mediterranean, and middle and low latitude of
318 Asia), increasing the OH- or NO₃-initiated oxidation pathways reduces the burden of limonene-derived
319 ON. This occurs because the oxidation of limonene by OH or NO₃ suppresses O₃-initiated oxidation,
320 which otherwise produces limonene-derived ON with a high yield. Additionally, if limonene undergoes
321 oxidation by NO₃, the availability of NO₃ for the nitration of OH- and O₃-initiated oxidation products of
322 limonene will decrease, resulting in a reduction in limonene-derived ON. The addition of OH- and O₃-
323 initiated oxidation pathways reduces global average burden of limonene-derived ON by 60.5% and 78.1%
324 respectively, compared to the case with NO₃-initiated oxidation pathway alone (Fig. S10e, f). This
325 reduction is likely due to insufficient NO₃ oxidation at night to further oxidize intermediates produced
326 from OH- and O₃-initiated limonene oxidation during the day, limiting the formation of limonene-derived
327 ON at night.

328 The burden of limonene-derived ON undergoes a noticeable change when an additional oxidation
329 pathway is introduced to the existing two pathways (Fig. S11). Adding OH-initiated oxidation pathway
330 increases the global average burden of limonene-derived ON from 41.8 to 60.5 $\mu\text{g}\cdot\text{m}^{-2}$, by 44.7%, while
331 adding O₃-initiated oxidation pathway decrease that from 75.5 to 60.5 $\mu\text{g}\cdot\text{m}^{-2}$, by 19.9% (Fig. S11a, b),
332 which was attributed to the competition between the OH and O₃ oxidation pathways for reactions with
333 limonene. When the O₃-initiated oxidation pathway produces the same amount of limonene-derived ON
334 as the OH-initiated pathway, it consumes more NO₃. As a result, increasing the O₃ oxidation pathway
335 reduces the availability of NO₃ for the nitration of intermediate oxidation products, thereby lowering the



total limonene-derived ON yield across all three pathways. In contrast, enhancing the OH oxidation pathway increases the total yield. Moreover, the addition of the NO₃-initiated oxidation pathway increases burden of limonene-derived ON in the limonene-sufficient region even over 150 µg·m⁻² (Fig. S11c). However, in the region with high NO₃ concentration, the burden of limonene-derived ON decreases (Fig. S11c) because the NO₃-initiated oxidation pathway yields less limonene-derived ON than the O₃- and OH-initiated oxidation pathways. These results highlight the different nonlinear responses of limonene-derived ON to multiple oxidation pathways under varying oxidation conditions and precursor concentrations. This difference contributes to the disparity between the global model results and the idealized experimental results from the box model, emphasizing the importance of developing explicit chemical mechanisms in global models for understanding SOA formation processes.

4 Conclusion and implications

In this work, the explicit chemical mechanism is developed to simulate formation and spatial distribution of limonene-derived ON using a chemical box model and global model CESM/IMPACT. Under multiple initial oxidation pathways, limonene-derived ON shows non-linear variations with different oxidant conditions, which is controlled by the synergetic effects of multiple oxidants. When limonene is not consumed, adding another oxidant with oxidation pathway will increase limonene-derived ON due to increased consumption of limonene. When limonene is completely consumed, limonene-derived ON production is dominated by competition of oxidation pathways. The production of limonene-derived ON is increased by O₃-initiated oxidation pathway while decreased by OH and NO₃-initiated oxidation pathway. This is mainly because limonene oxidated by O₃ produces more ON than OH and NO₃, resulting from the simulation under individual initial oxidation pathway.

The global model simulation indicates that oxidation process is important for limonene-derived ON formation in addition to limonene concentration. Global limonene-derived ON burden decreases by 19.9% and 17.3% due to O₃- and NO₃-initiated oxidation pathway, while OH-initiated oxidation pathway increases global limonene-derived ON burden by 44.7% compared the case only including the other two oxidation pathways. These differences can be attributed to the complex nonlinear response of limonene-derived ON yield to different reaction pathways under varying precursor and oxidant conditions.



363 The chemical mechanism of ON formation could have an influence on the formation and spatial
364 distribution of ON. We only include main oxidation process published to date in the model. Although
365 uncertainties remain in simulating limonene-derived ON due to limited knowledge of its formation
366 mechanism, this work offers an improvement in the global model's ability to simulate ON and presents
367 a methodological framework for simulating SOA and their chemical processes. This framework can be
368 used in the future to improve SOA burden predictions and provide a comprehensive understanding of the
369 complex interactions between multiple oxidation pathways, which are crucial for SOA formation (Chen
370 et al., 2022; Zang et al., 2024). Quantitative understanding of these complex interactions in contributing
371 to SOA formation is essential for understanding the contributions of interaction between anthropogenic
372 and natural emissions to atmospheric aerosols, and for providing more effective measures to reduce
373 aerosol pollution.

374 **Data availability.** Simulation data are available upon request to the corresponding authors.

375 **Author contributions.** QG and JZ designed the study, developed the chemical box model and global
376 model conducted the simulations, analyzed the data, and wrote the manuscript. HZ and BL provided the
377 laboratory data. PF, LC, YS, HL, YL and YX contributed to the discussion and revision of the paper.

378 **Competing interests.** The authors declare no competing financial interest.

379 **Disclaimer.** Publisher's note: Copernicus Publications remains neutral with regard to jurisdictional
380 claims in published maps and institutional affiliations.

381 **Acknowledgments.** The authors acknowledge the financial support of the National Natural Science
382 Foundation of China.

383 **Financial support.** This study was supported by the National Natural Science Foundation of China
384 (Grant 42177082).



385 **References**

- 386 Barber, V. P., Pandit, S., Green, A. M., Trongsiwat, N., Walsh, P. J., Klippenstein, S. J., and Lester, M.
387 I.: Four-Carbon Criegee Intermediate from Isoprene Ozonolysis: Methyl Vinyl Ketone Oxide Synthesis,
388 Infrared Spectrum, and OH Production, *J. Am. Chem. Soc.*, 140, 10866-10880,
389 <https://doi.org/10.1021/jacs.8b06010>, 2018.
- 390 Brown, S. S. and Stutz, J.: Nighttime Radical Observations and Chemistry, *Chem Soc Rev*, 41, 6405-
391 6447, <https://doi.org/10.1039/c2cs35181a>, 2012.
- 392 Capouet, M. and Müller, J. F.: A Group Contribution Method for Estimating the Vapour Pressures of α -
393 pinene Oxidation Products, *Atmos. Chem. Phys.*, 6, 1455-1467, [https://doi.org/10.5194/acp-6-1455-](https://doi.org/10.5194/acp-6-1455-2006)
394 [2006](https://doi.org/10.5194/acp-6-1455-2006), 2006.
- 395 Chen, Y., Tan, Y., Zheng, P., Wang, Z., Zou, Z., Ho, K. F., Lee, S., and Wang, T.: Effect of NO₂ on
396 Nocturnal Chemistry of Isoprene: Gaseous Oxygenated Products and Secondary Organic Aerosol
397 Formation, *Sci. Total Environ.*, 842, 156908, <https://doi.org/10.1016/j.scitotenv.2022.156908>, 2022.
- 398 Collaborators, G. B. D. R. F.: Global burden and strength of evidence for 88 risk factors in 204 countries
399 and 811 subnational locations, 1990-2021: a systematic analysis for the global burden of disease study
400 2021, *Lancet*, 403, 2162-2203, [https://doi.org/10.1016/S0140-6736\(24\)00933-4](https://doi.org/10.1016/S0140-6736(24)00933-4), 2024.
- 401 Compernelle, S., Ceulemans, K., and Müller, J. F.: EVAPORATION: a new vapour pressure estimation
402 method for organic molecules including non-additivity and intramolecular interactions, *Atmos. Chem.*
403 *Phys.*, 11, 9431-9450, <https://doi.org/10.5194/acp-11-9431-2011>, 2011.
- 404 Draper, D. C., Myllys, N., Hyttinen, N., Möller, K. H., Kjaergaard, H. G., Fry, J. L., Smith, J. N., and
405 Kurtén, T.: Formation of Highly Oxidized Molecules from NO₃ Radical Initiated Oxidation of Δ -3-
406 Carene: A Mechanistic Study, *ACS Earth Space Chem.*, 3, 1460-1470,
407 <https://doi.org/10.1021/acsearthspacechem.9b00143>, 2019.
- 408 Ehn, M., Thornton, J. A., Kleist, E., Sipila, M., Junninen, H., Pullinen, I., Springer, M., Rubach, F.,
409 Tillmann, R., Lee, B., Lopez-Hilfiker, F., Andres, S., Acir, I. H., Rissanen, M., Jokinen, T.,
410 Schobesberger, S., Kangasluoma, J., Kontkanen, J., Nieminen, T., Kurten, T., Nielsen, L. B., Jorgensen,
411 S., Kjaergaard, H. G., Canagaratna, M., Maso, M. D., Berndt, T., Petaja, T., Wahner, A., Kerminen, V.
412 M., Kulmala, M., Worsnop, D. R., Wildt, J., and Mentel, T. F.: A Large Source of Low-Volatility
413 Secondary Organic Aerosol, *Nature*, 506, 476-479, <https://doi.org/10.1038/nature13032>, 2014.
- 414 Farmer, D. K., Matsunaga, A., Docherty, K. S., Surratt, J. D., Seinfeld, J. H., Ziemann, P. J., and Jimenez,
415 J. L.: Response of an Aerosol Mass Spectrometer to Organonitrates and Organosulfates and Implications
416 for Atmospheric Chemistry, *Proc. Natl. Acad. Sci. U.S.A.*, 107, 6670-6675,
417 <https://doi.org/10.1073/pnas.0912340107>, 2010.
- 418 Fisher, J. A., Jacob, D. J., Travis, K. R., Kim, P. S., Marais, E. A., Miller, C. C., Yu, K., Zhu, L., Yantosca,
419 R. M., Sulprizio, M. P., Mao, J., Wennberg, P. O., Crounse, J. D., Teng, A. P., Nguyen, T. B., St Clair, J.
420 M., Cohen, R. C., Romer, P., Nault, B. A., Wooldridge, P. J., Jimenez, J. L., Campuzano-Jost, P., Day, D.
421 A., Hu, W., Shepson, P. B., Xiong, F., Blake, D. R., Goldstein, A. H., Misztal, P. K., Hanisco, T. F., Wolfe,
422 G. M., Ryerson, T. B., Wisthaler, A., and Mikoviny, T.: Organic Nitrate Chemistry and Its Implications
423 for Nitrogen Budgets in An Isoprene- and Monoterpene-Rich Atmosphere: Constraints from Aircraft
424 (SEAC⁴RS) and Ground-Based (SOAS) Observations in the Southeast US, *Atmos. Chem. Phys.*, 16,
425 5969-5991, <https://doi.org/10.5194/acp-16-5969-2016>, 2016.
- 426 Fry, J. L., Draper, D. C., Barsanti, K. C., Smith, J. N., Ortega, J., Winkler, P. M., Lawler, M. J., Brown,
427 S. S., Edwards, P. M., Cohen, R. C., and Lee, L.: Secondary Organic Aerosol Formation and Organic
428 Nitrate Yield from NO₃ Oxidation of Biogenic Hydrocarbons, *Environ. Sci. Technol.*, 48, 11944-11953,



- 429 <https://doi.org/10.1021/es502204x>, 2014.
- 430 Fry, J. L., Kiendler-Scharr, A., Rollins, A. W., Brauers, T., Brown, S. S., Dorn, H. P., Dubé, W. P., Fuchs,
431 H., Mensah, A., Rohrer, F., Tillmann, R., Wahner, A., Wooldridge, P. J., and Cohen, R. C.: SOA from
432 Limonene: Role of NO₃ in Its Generation and Degradation, *Atmos. Chem. Phys.*, 11, 3879-3894,
433 <https://doi.org/10.5194/acp-11-3879-2011>, 2011.
- 434 Glasius, M. and Goldstein, A. H.: Recent Discoveries and Future Challenges in Atmospheric Organic
435 Chemistry, *Environ. Sci. Technol.*, 50, 2754-2764, <https://doi.org/10.1021/acs.est.5b05105>, 2016.
- 436 Guenther, A. B., Jiang, X., Heald, C. L., Sakulyanontvittaya, T., Duhl, T., Emmons, L. K., and Wang, X.:
437 The Model of Emissions of Gases and Aerosols from Nature version 2.1 (MEGAN2.1): an Extended and
438 Updated Framework for Modeling Biogenic Emissions, *Geosci. Model Dev.*, 5, 1471-1492,
439 <https://doi.org/10.5194/gmd-5-1471-2012>, 2012.
- 440 Guo, F., Bui, A. A. T., Schulze, B. C., Dai, Q., Yoon, S., Shrestha, S., Wallace, H. W., Sanchez, N. P.,
441 Alvarez, S., Erickson, M. H., Sheesley, R. J., Usenko, S., Flynn, J., and Griffin, R. J.: Airmass History,
442 Night-Time Particulate Organonitrates, and Meteorology Impact Urban SOA Formation Rate, *Atmos.*
443 *Environ.*, 322, <https://doi.org/10.1016/j.atmosenv.2024.120362>, 2024.
- 444 Guo, Y., Shen, H., Pullinen, I., Luo, H., Kang, S., Vereecken, L., Fuchs, H., Hallquist, M., Acir, I.-H.,
445 Tillmann, R., Rohrer, F., Wildt, J., Kiendler-Scharr, A., Wahner, A., Zhao, D., and Mentel, T. F.:
446 Identification of Highly Oxygenated Organic Molecules and Their Role in Aerosol Formation in the
447 Reaction of Limonene with Nitrate Radical, *Atmos. Chem. Phys.*, 22, 11323-11346,
448 <https://doi.org/10.5194/acp-22-11323-2022>, 2022.
- 449 Hallquist, M., Wängberg, I., Ljungström, E., Barnes, I., and Becker, K.-H.: Aerosol and Product Yields
450 from NO₃ Radical-Initiated Oxidation of Selected Monoterpenes, *Environ. Sci. Technol.*, 33, 553-559,
451 <https://doi.org/10.1021/es980292s>, 1999.
- 452 Jokinen, T., Berndt, T., Makkonen, R., Kerminen, V. M., Junninen, H., Paasonen, P., Stratmann, F.,
453 Herrmann, H., Guenther, A. B., Worsnop, D. R., Kulmala, M., Ehn, M., and Sipilä, M.: Production of
454 Extremely Low Volatile Organic Compounds from Biogenic Emissions: Measured Yields and
455 Atmospheric Implications, *Proc. Natl. Acad. Sci. U.S.A.*, 112, 7123-7128,
456 <https://doi.org/10.1073/pnas.1423977112>, 2015.
- 457 Kiendler - Scharr, A., Mensah, A. A., Friese, E., Topping, D., Nemitz, E., Prevot, A. S. H., Äijälä, M.,
458 Allan, J., Canonaco, F., Canagaratna, M., Carbone, S., Crippa, M., Dall'Osto, M., Day, D. A., De Carlo,
459 P., Di Marco, C. F., Elbern, H., Eriksson, A., Freney, E., Hao, L., Herrmann, H., Hildebrandt, L., Hillamo,
460 R., Jimenez, J. L., Laaksonen, A., McFiggans, G., Mohr, C., O'Dowd, C., Otjes, R., Ovadnevaite, J.,
461 Pandis, S. N., Poulain, L., Schlag, P., Sellegri, K., Swietlicki, E., Tiitta, P., Vermeulen, A., Wahner, A.,
462 Worsnop, D., and Wu, H. C.: Ubiquity of Organic Nitrates from Nighttime Chemistry in the European
463 Submicron Aerosol, *Geophys. Res. Lett.*, 43, 7735-7744, <https://doi.org/10.1002/2016gl069239>, 2016.
- 464 Kilgour, D. B., Jernigan, C. M., Zhou, S., Brito de Azevedo, E., Wang, J., Zawadowicz, M. A., and
465 Bertram, T. H.: Contribution of Speciated Monoterpenes to Secondary Aerosol in the Eastern North
466 Atlantic, *ACS Environ. Sci. Technol. Air*, 555-566, <https://doi.org/10.1021/acsestair.3c00112>, 2024.
- 467 Kurten, T., Moller, K. H., Nguyen, T. B., Schwantes, R. H., Misztal, P. K., Su, L., Wennberg, P. O., Fry,
468 J. L., and Kjaergaard, H. G.: Alkoxy Radical Bond Scissions Explain the Anomalous Low Secondary
469 Organic Aerosol and Organonitrate Yields From α -Pinene + NO₃, *J. Phys. Chem. Lett.*, 8, 2826-2834,
470 <https://doi.org/10.1021/acs.jpcclett.7b01038>, 2017.
- 471 Kwan, A. J., Chan, A. W. H., Ng, N. L., Kjaergaard, H. G., Seinfeld, J. H., and Wennberg, P. O.: Peroxy
472 Radical Chemistry and OH Radical Production during the NO₃-Initiated Oxidation of Isoprene, *Atmos.*



- 473 Chem. Phys., 12, 7499-7515, <https://doi.org/10.5194/acp-12-7499-2012>, 2012.
- 474 Lelieveld, J., Evans, J. S., Fnais, M., Giannadaki, D., and Pozzer, A.: The contribution of outdoor air
475 pollution sources to premature mortality on a global scale, *Nature*, 525, 367-371,
476 <https://doi.org/10.1038/nature15371>, 2015.
- 477 Leungsakul, S., Jaoui, M., and Kamens, R. M.: Kinetic Mechanism for Predicting Secondary Organic
478 Aerosol Formation from the Reaction of d-Limonene with Ozone, *Environ. Sci. Technol.*, 39, 9583-9594,
479 <https://doi.org/10.1021/es0492687>, 2005.
- 480 Li, Y., Fu, T. M., Yu, J. Z., Yu, X., Chen, Q., Miao, R., Zhou, Y., Zhang, A., Ye, J., Yang, X., Tao, S., Liu,
481 H., and Yao, W.: Dissecting the Contributions of Organic Nitrogen Aerosols to Global Atmospheric
482 Nitrogen Deposition and Implications for Ecosystems, *Natl. Sci. Rev.*,
483 <https://doi.org/10.1093/nsr/nwad244>, 2023a.
- 484 Li, Y., Fu, T. M., Yu, J. Z., Yu, X., Chen, Q., Miao, R., Zhou, Y., Zhang, A., Ye, J., Yang, X., Tao, S., Liu,
485 H., and Yao, W.: Dissecting the contributions of organic nitrogen aerosols to global atmospheric nitrogen
486 deposition and implications for ecosystems, *Natl. Sci. Rev.*, 10, 244,
487 <https://doi.org/10.1093/nsr/nwad244>, 2023b.
- 488 Liu, D., Zhang, Y., Zhong, S., Chen, S., Xie, Q., Zhang, D., Zhang, Q., Hu, W., Deng, J., Wu, L., Ma, C.,
489 Tong, H., and Fu, P.: Large Differences of Highly Oxygenated Organic Molecules (HOMs) and Low-
490 Volatile Species in Secondary Organic Aerosols (SOAs) Formed from Ozonolysis of β -pinene and
491 Limonene, *Atmos. Chem. Phys.*, 23, 8383-8402, <https://doi.org/10.5194/acp-23-8383-2023>, 2023.
- 492 Luo, H., Vereecken, L., Shen, H., Kang, S., Pullinen, I., Hallquist, M., Fuchs, H., Wahner, A., Kiendler-
493 Scharr, A., Mentel, T. F., and Zhao, D.: Formation of Highly Oxygenated Organic Molecules from the
494 Oxidation of Limonene by OH Radical: Significant Contribution of H-abstraction Pathway, *Atmos.*
495 *Chem. Phys.*, 23, 7297-7319, <https://doi.org/10.5194/acp-23-7297-2023>, 2023.
- 496 Matsunaga, A. and Ziemann, P. J.: Branching Ratios and Rate Constants for Decomposition and
497 Isomerization of beta-Hydroxyalkoxy Radicals Formed from OH Radical-Initiated Reactions of C₆-C₁₃
498 2-Methyl-1-Alkenes in the Presence of NO_x, *J Phys Chem A*, 123, 7839-7846,
499 <https://doi.org/10.1021/acs.jpca.9b06218>, 2019.
- 500 Mayorga, R., Xia, Y., Zhao, Z., Long, B., and Zhang, H.: Peroxy Radical Autoxidation and Sequential
501 Oxidation in Organic Nitrate Formation during Limonene Nighttime Oxidation, *Environ. Sci. Technol.*,
502 15337-15346, <https://doi.org/10.1021/acs.est.2c04030>, 2022.
- 503 Moldanova, J. and Ljungström, E.: Modelling of Particle Formation from NO₃ Oxidation of Selected
504 Monoterpenes, *J. Aerosol Sci.*, 31, 1317-1333, [https://doi.org/10.1016/S0021-8502\(00\)00041-0](https://doi.org/10.1016/S0021-8502(00)00041-0), 2000.
- 505 Ng, N. L., Brown, S. S., Archibald, A. T., Atlas, E., Cohen, R. C., Crowley, J. N., Day, D. A., Donahue,
506 N. M., Fry, J. L., Fuchs, H., Griffin, R. J., Guzman, M. I., Herrmann, H., Hodzic, A., Iinuma, Y., Jimenez,
507 J. L., Kiendler-Scharr, A., Lee, B. H., Luecken, D. J., Mao, J., McLaren, R., Mutzel, A., Osthoff, H. D.,
508 Ouyang, B., Picquet-Varraut, B., Platt, U., Pye, H. O. T., Rudich, Y., Schwantes, R. H., Shiraiwa, M.,
509 Stutz, J., Thornton, J. A., Tilgner, A., Williams, B. J., and Zaveri, R. A.: Nitrate Radicals and Biogenic
510 Volatile Organic Compounds: Oxidation, Mechanisms, and Organic Aerosol, *Atmos. Chem. Phys.*, 17,
511 2103-2162, <https://doi.org/10.5194/acp-17-2103-2017>, 2017.
- 512 Pankow, J. F. and Asher, W. E.: SIMPOL.1: a simple group contribution method for predicting vapor
513 pressures and enthalpies of vaporization of multifunctional organic compounds, *Atmos. Chem. Phys.*, 8,
514 2773-2796, <https://doi.org/10.5194/acp-8-2773-2008>, 2008.
- 515 Perring, A. E., Pusede, S. E., and Cohen, R. C.: An Observational Perspective on the Atmospheric
516 Impacts of Alkyl and Multifunctional Nitrates on Ozone and Secondary Organic Aerosol, *Chem. Rev.*,



- 113, 5848-5870, <https://doi.org/10.1021/cr300520x>, 2013.
- Pye, H. O., Luecken, D. J., Xu, L., Boyd, C. M., Ng, N. L., Baker, K. R., Ayres, B. R., Bash, J. O., Baumann, K., Carter, W. P., Edgerton, E., Fry, J. L., Hutzell, W. T., Schwede, D. B., and Shepson, P. B.: Modeling the Current and Future Roles of Particulate Organic Nitrates in the Southeastern United States, *Environ. Sci. Technol.*, 49, 14195-14203, <https://doi.org/10.1021/acs.est.5b03738>, 2015.
- Rollins, A. W., Kiendler-Scharr, A., Fry, J. L., Brauers, T., Brown, S. S., Dorn, H. P., Dubé, W. P., Fuchs, H., Mensah, A., Mentel, T. F., Rohrer, F., Tillmann, R., Wegener, R., Wooldridge, P. J., and Cohen, R. C.: Isoprene Oxidation by Nitrate Radical: Alkyl Nitrate and Secondary Organic Aerosol Yields, *Atmos. Chem. Phys.*, 9, 6685-6703, <https://doi.org/10.5194/acp-9-6685-2009>, 2009.
- Sato, K., Inomata, S., Xing, J.-H., Imamura, T., Uchida, R., Fukuda, S., Nakagawa, K., Hirokawa, J., Okumura, M., and Tohno, S.: Effect of OH Radical Scavengers on Secondary Organic Aerosol Formation from Reactions of Isoprene with Ozone, *Atmos. Environ.*, 79, 147-154, <https://doi.org/10.1016/j.atmosenv.2013.06.036>, 2013.
- Shen, H., Zhao, D., Pullinen, I., Kang, S., Vereecken, L., Fuchs, H., Acir, I. H., Tillmann, R., Rohrer, F., Wildt, J., Kiendler-Scharr, A., Wahner, A., and Mentel, T. F.: Highly Oxygenated Organic Nitrates Formed from NO₃ Radical-Initiated Oxidation of beta-Pinene, *Environ. Sci. Technol.*, 55, 15658-15671, <https://doi.org/10.1021/acs.est.1c03978>, 2021.
- Sindelarova, K., Granier, C., Bouarar, I., Guenther, A., Tilmes, S., Stavrou, T., Müller, J. F., Kuhn, U., Stefani, P., and Knorr, W.: Global Data Set of Biogenic VOC Emissions Calculated by the MEGAN Model over the last 30 years, *Atmos. Chem. Phys.*, 14, 9317-9341, <https://doi.org/10.5194/acp-14-9317-2014>, 2014.
- Spittler, M., Barnes, I., Bejan, I., Brockmann, K. J., Benter, T., and Wirtz, K.: Reactions of NO₃ Radicals with Limonene and α -pinene: Product and SOA Formation, *Atmos. Environ.*, 40, 116-127, <https://doi.org/10.1016/j.atmosenv.2005.09.093>, 2006.
- Surratt, J. D., Gómez-González, Y., Chan, A. W. H., Reinhilde, V., Mona, S., E, K. T., O, E. E., H, O. J., Michael, L., Mohammed, J., Willy, M., Magda, C., C, F. R., and H, S. J.: Organosulfate Formation in Biogenic Secondary Organic Aerosol, *J. Phys. Chem. A*, 112, <https://doi.org/10.1021/jp802310p>, 2008.
- Tao, J., Zhang, L., Cao, J., and Zhang, R.: A review of current knowledge concerning PM_{2.5} chemical composition, aerosol optical properties and their relationships across China, *Atmos. Chem. Phys.*, 17, 9485-9518, <https://doi.org/10.5194/acp-17-9485-2017>, 2017.
- Wang, L. and Wang, L.: The oxidation mechanism of gas-phase ozonolysis of limonene in the atmosphere, *Phys Chem Chem Phys*, 23, 9294-9303, <https://doi.org/10.1039/d0cp05803c>, 2021.
- Xu, L., Tsona, N. T., You, B., Zhang, Y., Wang, S., Yang, Z., Xue, L., and Du, L.: NO_x Enhances Secondary Organic Aerosol Formation from Nighttime γ -terpinene Ozonolysis, *Atmos. Environ.*, 225, <https://doi.org/10.1016/j.atmosenv.2020.117375>, 2020.
- Yu, K., Zhu, Q., Du, K., and Huang, X.-F.: Characterization of Nighttime Formation of Particulate Organic Nitrates Based on High-Resolution Aerosol Mass Spectrometry in an Urban Atmosphere in China, *Atmos. Chem. Phys.*, 19, 5235-5249, <https://doi.org/10.5194/acp-19-5235-2019>, 2019.
- Zang, H., Luo, Z., Li, C., Li, Z., Huang, D., and Zhao, Y.: Nocturnal Atmospheric Synergistic Oxidation Reduces the Formation of Low-Volatility Organic Compounds from Biogenic Emissions, *Atmos. Chem. Phys.*, 24, 11701-11716, <https://doi.org/10.5194/acp-24-11701-2024>, 2024.
- Zare, A., Fahey, K. M., Sarwar, G., Cohen, R. C., and Pye, H. O. T.: Vapor-Pressure Pathways Initiate but Hydrolysis Products Dominate the Aerosol Estimated from Organic Nitrates, *ACS Earth Space Chem.*, 3, 1426-1437, <https://doi.org/10.1021/acsearthspacechem.9b00067>, 2019.



561 Zhao, D. F., Kaminski, M., Schlag, P., Fuchs, H., Acir, I. H., Bohn, B., Häsel, R., Kiendler-Scharr, A.,
562 Rohrer, F., Tillmann, R., Wang, M. J., Wegener, R., Wildt, J., Wahner, A., and Mentel, T. F.: Secondary
563 Organic Aerosol Formation from Hydroxyl Radical Oxidation and Ozonolysis of Monoterpenes, Atmos.
564 Chem. Phys., 15, 991-1012, <https://doi.org/10.5194/acp-15-991-2015>, 2015.

565

566

567

568

569

570

571